Metabolic Engineering 60 (2020) 77–86

Contents lists available at ScienceDirect

Metabolic Engineering

journal homepage: www.elsevier.com/locate/meteng

Transient vitamin B5 starving improves mammalian cell homeostasis and protein production

Lucille Pourcel[a,*], Flavien Buron[a], Fanny Garcia[a], Margaux-Sarah Delaloix[a], Valérie Le Fourn[b], Pierre-Alain Girod[b], Nicolas Mermod[a]

[a] Center for Biotechnology and Department of Fundamental Microbiology, University of Lausanne, UNIL-EPFL, Lausanne, Switzerland
[b] Selexis SA, 18 Ch. des Aulx, Geneva, Switzerland

ARTICLE INFO

Keywords:
Vitamin B5
SLC5A6 transporter
PPAR
Metabolic homeostasis
Mammalian cells

ABSTRACT

Maintaining a metabolic steady state is essential for an organism's fitness and survival when confronted with environmental stress, and metabolic imbalance can be reversed by exposing the organism to fasting. Here, we attempted to apply this physiological principle to mammalian cell cultures to improve cellular fitness and consequently their ability to express recombinant proteins. We showed that transient vitamin B5 deprivation, an essential cofactor of central cellular metabolism, can quickly and irreversibly affect mammalian cell growth and division. A selection method was designed that relies on mammalian cell dependence on vitamin B5 for energy production, using the co-expression of the B5 transporter SLC5A6 and a gene of interest. We demonstrated that vitamin B5 selection persistently activates peroxisome proliferator-activated receptors (PPAR), a family of transcription factors involved in energy homeostasis, thereby altering lipid metabolism, improving cell fitness and therapeutic protein production. Thus, stable PPAR activation may constitute a cellular memory of past deprivation state, providing increased resistance to further potential fasting events. In other words, our results imply that cultured cells, once exposed to metabolic starvation, may display an improved metabolic fitness as compared to non-exposed cells, allowing increased resistance to cellular stress.

1. Introduction

Large amounts of active protein are usually required for functional and structural analysis, as well as for the production of biological therapeutics. For most eukaryotic proteins, this also requires homogeneous post-translational modifications, as can be achieved by expression in cultured mammalian cells. Optimization of gene transfer methods, selection process, protein synthesis and culture conditions are currently performed to obtain higher yields of recombinant proteins from stably transfected mammalian cells. Nevertheless, despite significant progress, the protein production rate appears to be limited by intrinsic metabolic bottlenecks in the cells and by the production of toxic metabolic by-products such as lactate. Changes in the central metabolism of cultured cells highlighted a regulatory link between metabolite cellular intake, cell growth and recombinant protein production (Dean and Reddy, 2013). Moreover, the maintenance of an organism's metabolic steady state, also termed energy homeostasis, is essential for its fitness and survival when confronted with environmental stresses such as starvation, infections or injuries (Kotas and Medzhitov, 2015). A metabolic unbalance can occur after changes in nutrient diet, which may activate alternative metabolic pathways in order to return to a balanced energy state. For instance, the liver maintains energy homeostasis during fasting by activation of ketogenesis, to provide enough energy-yielding nutrients for critical organs such as brain and muscles (van den Berghe, 1991). In such conditions, the hepatic acetyl-CoA, a key molecule in central metabolism, will be converted into ketones instead of entering the TCA cycle (Pietrocola et al., 2015). These ketones will then enter blood circulation to be taken up into extra-hepatic cells, reconverted into acetyl-CoA and metabolized by the TCA cycle for ATP production (Puchalska and Crawford, 2017).

The peroxisome proliferator-activated receptors (PPARs) are ligand-activated transcription factors that belong to the superfamily of nuclear hormone receptors and play an essential role in energy homeostasis, cell proliferation and differentiation (Kersten et al., 2000). Three different PPAR subtypes have been identified, termed PPARα, PPARβ/δ and PPARγ. Fatty acids and derivatives produced in hepatic cells during starvation activate PPARα, which will in turn induce the transcription of target genes involved in ketogenesis, lipid metabolism and anti-inflammatory response (Kersten et al., 2000; Rakhshandehroo et al.,

* Corresponding author. Center for Biotechnology and Department of Fundamental Microbiology, University of Lausanne, UNIL-EPFL, Lausanne, Switzerland
E-mail address: Lucille.Pourcel@sib.swiss (L. Pourcel).

https://doi.org/10.1016/j.ymben.2020.03.008
Received 28 May 2019; Received in revised form 23 January 2020; Accepted 22 March 2020
Available online 02 April 2020

2010). Recent studies have demonstrated that activating the PPAR signalling pathway in mammals, either by caloric restriction or by increasing the proportion of fatty acid-derived products such as ketones in the diet, leads to the reduction in oxidative damage and to the induction of autophagy to modulate nutrient recycling. These fasting-induced mechanisms were shown to improve mammalian lifespan and general fitness (Lee et al., 2014; Newman et al., 2017; Redman et al., 2018). Although the beneficial impacts of activating the PPAR pathway are well described in organisms, the possible occurrence of such fasting-induced long-term effects have not been studied at the cell culture level. Moreover, attempts to characterize key components of energy metabolism regulation in cultured cells, a necessary step to engineering their central metabolism to possibly improve recombinant protein production, have not been reported.

Here, we hypothesized that cultured mammalian cells subjected to nutrient depletion, therefore mimicking a state of fasting, might display the beneficial properties of improved fitness observed in animals. We assessed whether stressed-cells could develop a selective advantage due to the activation of alternative metabolic pathways, leading to improved energy homeostasis. To do so, we designed a metabolic selection approach based on vitamin B5 deficiency, given the central role of vitamins in cell metabolism and the severe metabolic stress and diseases elicited by their deprivation (Kobayashi et al., 2011). We showed that overexpression of SLC5A6, a transporter mediating the uptake of vitamin B5 and biotin (Ghosal et al., 2013; Uchida et al., 2015), can be used to increase cell growth and viability in conditions of limiting B5 availability. A selection procedure based on SLC5A6 co-expression was established, yielding populations of CHO cells producing recombinant proteins at very high and homogeneous levels. Given the central role of vitamin B5 as an essential cofactor for acetyl-CoA biosynthesis, we deciphered the genetic and metabolic changes occurring in cells during B5 selection, to identify a set of PPARα-induced target genes. We show that transient B5-starvation leads to persistent PPARα activation in cultured cell populations, improving cell viability in a nutrient-limiting environment. PPARα activation was found to improve lipid homeostasis and to decrease the synthesis of toxic by-products such as lactate, improving the cell metabolic fitness, which was accompanied by increased production of proteins of interest. We conclude that B5 deprivation of CHO cell cultures leads to the establishment of a fasting state, which may overcome the metabolic bottlenecks limiting the expression of recombinant proteins by cultured cells.

2. Materials and methods

2.1. Vitamin gene sequences and DNA vector constructs

Genomic and cDNA sequences were determined after alignment of the homologous genes in mice using NCBI BLAST software. Chinese hamster ovary cells (CHO–K1) cDNAs were produced by reverse transcription from 1 μg of total RNA isolated from 10^6 cells (NucleoSpin™ RNA kit; Macherey-Nagel) using the GoScript Reverse transcription System (Promega).

Vectors were constructed as follow: The *SLC5A6* coding sequence was amplified from CHO cell cDNA library by PCR (PHUSION High-Fidelity DNA Polymerase; Thermo Fisher Scientific) using primers carrying restriction sites. The amplicon was cloned into the *pGAPDH-MAR 1-68-GFP* vector (Selexis Inc.), by cutting out the green fluorescent protein (*GFP*) sequence and replacing it with that of *SLC5A6*. The GFP protein was expressed using a eukaryotic expression cassette composed of a human cytomegalovirus (CMV) enhancer and human glyceraldehydes 3-phosphate dehydrogenase (GAPDH) promoter upstream of the GFP coding sequence followed by a simian virus 40 (SV40) polyadenylation signal, the human gastrin terminator and a SV40 enhancer (Le Fourn et al., 2014). The pSV-PURO vector contains the puromycin resistance gene under the control of the SV40 promoter originating from the pRc/RSVplasmid (Invitrogen). The blasticidin vector contains the blasticidin resistance gene under the control of the CMV promoter originating from the pCMV/Bsd plasmid (Invitrogen). The immunoglobulin expression vectors *pGAPDH-MAR1-68-IgG-Lc* and *pGAPDH-MAR1-68-IgG-Hc* expressing the trastuzumab monoclonal immunoglobulin (IgG) light chain (Lc) and heavy chain (Hc) were as previously described (Le Fourn et al., 2014). The TNFR-Fc and Infliximab expression vectors were cloned in the same mammalian expression vectors carrying the puromycin resistance gene.

2.2. Cell culture and stable transfections

CHO cells were maintained in suspension culture in SFM4CHO-M Hyclone serum-free medium (SFM, Thermo Fisher Scientific) supplemented with L-glutamine (PAA) and HT supplement (Gibco) at 37 °C, 5% CO2 in humidified air. Other cell media used for these experiments are the BalanCD CHO-M Growth A (B-CDfull; Irvine Scientific), and the Deficient BalanCD CHO-M Growth A (B-CDmin; Irvine Scientific), supplemented with vitamin B1 (thiamine Hydrochloride; Sigma-Aldrich), vitamin B5 (Calcium DL-Pantothenate; TC) and vitamin H (Biotin, Sigma-Aldrich). The BSO3 trastuzumab-expressing cell clone was generated as as the highest producing clone after several limiting dilution steps among 192 positive clones, as previously described (Le Fourn et al., 2014). Transfections were performed as follows: CHO cells were transformed with *PvuI*-digested expression vectors by electroporation according to the manufacturer's recommendations (Neondevices, Invitrogen). Production of stable cell lines was achieved using SFM4CHO complete media complemented with 7.5 μg/ml of blasticidin for 3 weeks for blasticidin selection, 10 mg/ml of puromycin for 9 days for puromycin selection, or with the B5 deficient media for B5 selection. B5 selection was performed as follows: One day before transfection, cells were grown at 300′000 cells/ml in B5 selective media which consisted in B-CDmin media supplemented with 7.5 μM B1 (1X), 2.5 nM B5 (10^{-3}X) and 50 pM H (10^{-4}X). After transfection, cells were incubated with B5 selective media for 9–14 days, and then transferred into SFM non-selective medium. For Puro/B5 double selection, polyclonal stable cell lines were first selected with alternance of 10 mg/ml of puromycin and B5 selective media (10^{-3}X B5/10^{-4}X H) for the indicated days, then transferred into SFM non-selective media. Stable clones were isolated by limited dilution or using Clonepix device.

2.3. Analyses of stable polyclonal and monoclonal lines

Fed-Batch Performance Evaluation: Growth and IgG secretion performances in fed-batch culture were performed according to Le Fourn et al. (Le Fourn et al., 2014), with the following changes: high IgG producing clones were seeded at 300′000 cells/ml in 5mL culture medium in falcon of 50 mL. Viable cell density and IgG titers, expressed as g/L of IgG in the cell culture supernatant, were evaluated after 3, 6, 8 10 and 13 days. TNFR-Fc expressing pools were sub-cultivated in 125 ml shake flasks in 20 ml of culture medium every 3–4 days. IgG titer in cell culture supernatants was measured by sandwich ELISA. *IgG cell surface staining*: Detection of cell surface IgG (i.e. surface staining) was based on protocol from Brezinsky et al., (Brezinsky et al., 2003), as described in Harraghy et al., (Harraghy et al., 2012), and modified as follows: labelling was performed in a 2mL Eppendorf tube, using an APC-conjugated antibody (Allophycocyanin (APC)-conjugated Affini-Pure Goat Anti-human IgG (Jackson ImmunoResearch). Moreover, cells were not fixed. Surface IgG display was assessed by FACS analysis using a flow cytometry (Beckman Coulter). *Single-cell cloning with ClonePix FL device*: Cell pools expressing recombinant IgG protein were subcloned using ClonePix™ FL Imager from Molecular Devices. Briefly a semi-solid media was prepared by mixing equal parts of liquid concentrate (2×) SFM4CHO medium containing L-glutamine and CloneMatrix™ (Molecular Devices). This mix was supplemented with the CloneDetect™ FITC reagent consisting anti-human IgG antibody conjugated to FITC. Cells were inoculated in this medium at 200 cells/ml in 6-well plates. Plates

were then incubated 10 days at 37 °C, 5% CO2, in a humidified incubator. Growing and secreting colonies were detected by Clonepix FL Imaging software. Highly-secreting colonies were picked and transferred to 96-well plates containing culture medium. The intensity of the secretion halo measured by Clonepix FL Imaging software was used to rank clones and illustrated producers distribution of tested and control pools. *Cell Secretion Assay*: The stable IgG expression of transfected CHO cell lines was analysed with Cell Secretion Assay and Celigo Cell Cytometer imaging (Celigo S Application, Nexcelom). Briefly, cells were incubated at 37 °C overnight, with a green-fluorescent cell detection reagent (CellTracker™ Green CMFDA Dye) and with an anti-human IgG PE-conjugated antibody. After overnight incubation, culture plates were imaged using CSA application of Celigo Cell Cytometer. The anti-human IgG PE-conjugated antibody interacts with the secreted recombinant protein by forming fluorescent detectable secretion network closer to the single cell – the halo of secretion. The % of secreting clones in polyclonal populations was used to assess the homogeneity of pools. The analysis of the intensity of the secretion halo was used to estimate the production level of the total population as well as to determine the distribution of high (HP), medium (MP) and low-producers subpopulations (LP). *GFP fluorescence*: The percentage of fluorescent cells and the fluorescence intensity of GFP positive cells were determined by FACS analysis using a CyAn ADP flow cytometer (Beckman Coulte).

2.4. Transient transfection assays of PPAR transcription factors activity

Transient transfection assays were performed as follows: CHO cells were transfected with PPRE-TK-DsRed (provided by Prof. Michalik, University of Lausanne), consisting of multiple copies of the PPAR response element (PPRE) fused to a minimal thymidine kinase (TK) promoter located upstream of the dsRed coding sequence, or with TK-DsRed devoid of the PPRE sequence, with or without the pSG5_PPARα expression vector (Issemann and Green, 1990). pE-BFP2-Nuc (2xNLS), used as internal transfection control, contains the eBFP2 (enhanced blue fluorescent protein 2) coding sequence and a nuclear localization sequence under the control of minimal CMV promoter (Addgene). Cell were observed 48 h after transfection by flow cytometry using a Gallios Flow Cytometer (Beckman Coulte) and the fluorescence was analysed by Kaluza Acquisition software. The DsRed fluorescence (638 nm) was standardized relative to that of the BFP2 marker (488 nm).

2.5. RNA PCR and sequencing analysis

For sequencing analysis, cells were grown for 4 days in spin-tubes without antibiotic selection. Total RNA was isolated from cells using the NucleoSpin RNA kit (Macherey-Nagel). RNA quality was evaluated using the Fragment Analyzer (Advanced Analytical). RNA-seq library preparation was performed using 0.5 μg–1 μg of total RNA converted to cDNA using the Illumina TruSeq stranded mRNA-seq reagents (Illumina). The RNA-seq library 100nt paired end was sequenced on the Illumina HiSeq 2500. Reads were mapped to the CHO–K1 transcriptome (Pruitt, 2014). Cells used for the RNASeq analysis were the following: 1) CHO cells; 2) Clones expressing the interferon beta and SLC5A6; selected with puromycin/B5, or with puromycin only 3) Polyclonal cell population expressing the trastuzumab and SLC5A6 selected with puromycin/B5, or with puromycin only. For real time quantitative PCR (RT-qPCR) analysis, total RNA was extracted from 10^6 cells and reverse transcribed into cDNA. Transcripts accumulation was quantified by RT-qPCR using the SYBR Green-Taq polymerase kit from Eurogentec Inc. and ABI Prism 7700 PCR machine (Applied Biosystems). Transcript levels were normalized to that of GAPDH housekeeping gene.

2.6. Metabolite analyses (metabolite extraction, sample amount normalization)

Metabolite extraction: For metabolite quantification, cell pellets were extracted with 1 mL of cold MeOH:H2O (4:1, v/v) solvent mixture as a best compromise to efficiently precipitate proteins, quench the metabolism and extract a broad range of polar metabolites. The samples were then probe-sonicated (4 pulses x 5 s) to lyse the cells completely and improve the metabolite extraction. To promote protein precipitation, the samples were incubated for 1 h at −20 °C, followed by 15 min centrifugation at 13,000 rpm at 4 °C. The resulting supernatants were collected and evaporated to dryness in a vacuum concentrator (LabConco). Then, the sample extracts were reconstituted in 100 μL MeOH:Water (4:1) and injected into the LC-MS system. *Protein quantification*: The protein pellets were evaporated and lysed in 20 mM Tris-HCl (pH 7.5), 4 M guanidine hydrochloride, 150 mM NaCl, 1 mM Na2EDTA, 1 mM EGTA, 1% Triton, 2.5 mM sodium pyrophosphate, 1 mM beta-glycerophosphate, 1 mM Na3VO4, 1 μg/ml leupeptin using brief probe-sonication (5 pulses x 5 s). The BCA Protein Assay Kit (Thermo Fisher Scientific) was used to measure total protein concentrations (Hidex). *Data acquisition – LC-HRMS*: Extracted samples were analysed by Hydrophilic Interaction Liquid Chromatography coupled to high resolution mass spectrometry (HILIC - HRMS) in negative ionization modes using a Q-Exactive instrument (Quadrupole Orbitrap mass spectrometer) (Thermo Fisher Scientific) operating at mass resolving power of 70,000 full width half maximum (FWHM). Metabolites were separated by chromatography using a ZIC pHILIC (100 mm, 2.1 mm I.D. and 5 μm particle size) column. The mobile phase was composed of A = 20 mM ammonium Acetate and 20 mM NH4OH in water at pH 9.3 and B = 100% ACN. The linear gradient elution from 90% B (0–1.5 min) down to 50% B was applied (1.5 min–8 min), followed by an isocratic step (8 min–11 min) and linear gradient down to 45% B (11 min–12 min). These conditions were held 3 min. Finally, the initial chromatographic conditions were established as a post-run during 9 min for column re-equilibration. The flow rate was 300 μL/min, column temperature 30 °C and sample injection volume 2.5 μl. ESI source conditions were set as follows: probe heater temperature 200 °C, sheath gas 60 a.u., auxiliary gas 15 a.u., capillary temperature 280 °C and ESI spray voltage −3600 V. Full scan mode was used as acquisition mode to quantify lactate, pyruvate, 3-hydroxybutyrate and pantothenic acid, while acetyl-CoA was quantified using parallel reaction monitoring (PRM) acquisition mode using 30 eV as collision energy. *Data processing*: Raw LC-HRMS data was processed using the Thermo Fisher Scientific software (Xcalibur 4.0 QuanBrowser, Thermo Fisher Scientific). Metabolite quantification was performed using external calibration curves.

2.7. Statistical analysis

The results are expressed as means ± standard error of the mean (SEM). Statistical analyses were performed using the Student's t-test, with variance equality depending on sample variance F-test. Asterisks in the figure panels refer to statistical probabilities p values of less than or equal to 0.05, which were considered as statistically significant.

3. Results and discussion

3.1. Determination of vitamin-limiting cell growth conditions

We chose to specifically focus on vitamins B5, H and B1, as they are involved in key mitochondrial functions for energy production (Ghosal et al., 2013; Lindhurst et al., 2006; Subramanian et al., 2012). To assess the effect of limiting the concentration of the vitamins on cell growth, we designed a cell culture medium specifically depleted of vitamins B5, H and B1, termed B-CDmin. CHO cells seeded in the B-CDmin medium were unable to maintain cell divisions, as expected (Fig. 1A). Over time, cell size was reduced, and cells started to lose viability after 6 days of incubation in the vitamin-lacking medium (Figs. S1A and S1B). The B-CDmin medium was next complemented with known amounts of the vitamins, setting standard B5, H and B1 concentrations (1X) at 2.5μM,

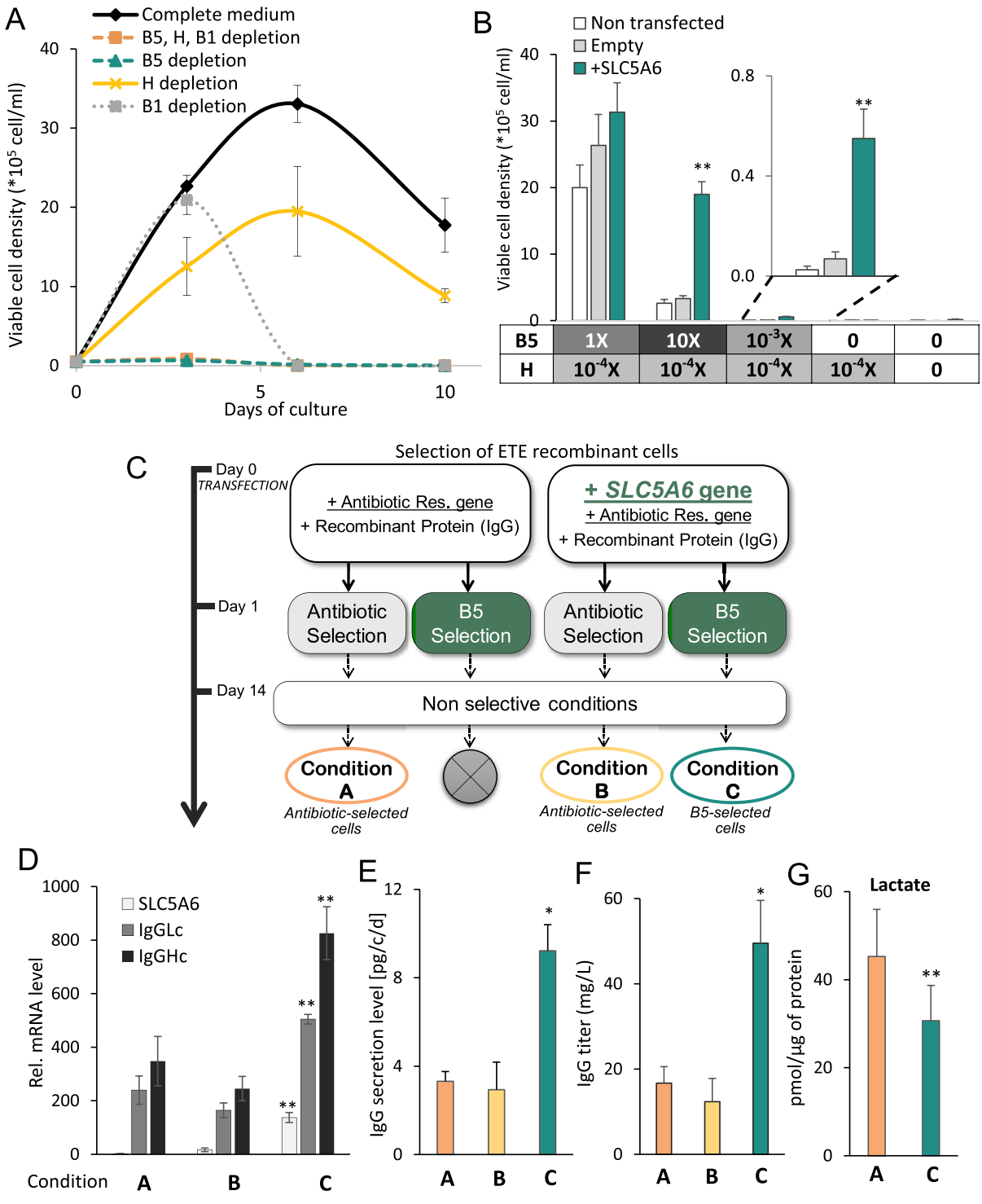

Fig. 1. CHO cells growth in vitamin-deficient media. (A) Cells were seeded in a B-CDmin medium supplemented or not with vitamin B1, B5 or H. Viable cell density was measured after at 3, 6 and 10 days of culture. (B) CHO cell were co-transfected with the SLC5A6 expression vector, or an empty vector control devoid of the SLC5A6 coding sequence, together with a puromycin resistance vectors, and polyclonal populations were selected for puromycin resistance. Cells were seeded in B-CDmin medium supplemented with the indicated amounts of vitamin B5 and H, and with B1 (1X). Viable cell density was measured after 6 days of culture. Non transfected cells and transfected cells without SLC5A6 vector (Empty) were used as controls. $^{**}P \leq 0.02$ (*t*-test; 2 tails) with respect to non-transfected cells within the same condition of growth and culture medium. Detailed control parameters for cultivations are given in Methods. (C) Experimental cell selection workflow. CHO cells were co-transfected without or with the *SLC5A6* expression vector, together with the ETE trastuzumab and the puromycin resistance vectors, after which cells were selected either in presence of puromycin (conditions A and B) or in the B5-deficient culture medium (condition C and B). After selection, cells were transferred to a non-selective culture medium. The crossed circle indicates that cells did not survive selection. (D) *SCL5A6* and IgG chains mRNA levels of cell pools A, B and C. Relative mRNA level was determined by RT-qPCR. $^{**}P \leq 0.02$ with respect to condition A (*t*-test; 2 tails). (E) IgG secretion assays of cell pools A, B and C, as represented by the specific productivity assayed by double sandwich ELISA. $^{*}P \leq 0.05$ with respect to condition A (*t*-test; 1 tail). (F) IgG titers from cell pools A, B and C, measured after 3 days-batch culture in non-selective medium. $^{*}P \leq 0.05$ with respect to condition A (*t*-test; 1 tail). (G) Lactate content in cell pools from A and C, after 6 days of a fed-batch culture, measured by LC-MS. $^{**}P \leq 0.02$ with respect to condition A (*t*-test; 2 tails). Data are mean values ± SEM from 3 replicates.

0.5μM and 7.5μM, respectively, as found in commonly used complete media. In the culture medium deprived solely of B5, cells did not divide, and viability decreased after 6 days, as in the B-CDmin medium. When either B1 or H was depleted, cells were able to divide for 3–6 days respectively, and growth was reduced overall as compared to the full media. Therefore, we concluded that B5 was most limiting for cell growth in the short term, as it must be present continuously in the culture medium to allow cell division.

Vitamin B5 shares a common single cytoplasmic transporter with vitamin H termed SLC5A6 (Fig. S1C). As competition of B5 and H transport may occur during vitamin uptake into the cell, we assessed cell division in culture media containing various concentrations of both vitamins. The B-CDmin medium was complemented with lower concentrations of each vitamin separately, to determine the concentration range limiting cell growth after 6 days of culture. Because B5 is most limiting for cell growth, we decreased H concentration by four orders of magnitude (10^{-4}X) to 50 pM, in order to increase the transporter availability for B5. In these conditions, B5 was essential for CHO cell growth, with a growth-limiting concentration range of B5 around 10^{-3}X (2.5 nM) and near-maximal growth at 1X (Figs. S1D and S1E). However, further addition of B5 up to a 10-fold excess inhibited cell growth, as expected from a competition between B5 and H for uptake by the SLC5A6 transporter. These findings implied that overexpression of the SLC5A6 transporter might provide an advantage to cells grown in a B5-limiting medium. This was assessed by generating polyclonal populations stably overexpressing *SLC5A6*, which were then grown in the B-CDmin medium supplemented with various concentrations of B5 and H (Fig. 1B). No significant growth difference was observed when comparing polyclonal cell lines cultured with 1X B5 and 10^{-4}X H upon overexpression of *SLC5A6*. As previously observed, cell division nearly stopped in the complete absence of B5 after 6 days of culture, irrespective of the overexpression of the transporter or in the presence of vitamin H. Interestingly, when excess B5 was added in the presence of the low H amount (10X B5/10^{-4}X H), cells overexpressing *SLC5A6* divided significantly more than control cells. This further indicated the occurrence of a competition of the two vitamins for their common transporter, where saturating concentrations of B5 may limit growth by inhibiting the uptake of low amounts of H in the culture medium, unless the transporter is overexpressed. More strikingly, cells transfected with the SLC5A6 expression vector reached significantly higher cell densities in B5 limiting condition (10^{-3}X B5/10^{-4}X H). Moreover, while cells without exogenous transporter overexpression did not survive culture in the B5-limiting medium, cells overexpressing SLC5A6 survived B5 deprivation, and they recovered a normal growth when further transferred into complete media (1X B5/1X H, data not showed). Overall, we concluded that overexpression of the SLC5A6 transporter can confer a growth advantage that is most significant in presence of either saturating concentrations of B5 (10X) and limiting amounts of H (10^{-4}X), or conversely in the presence of limiting concentrations of B5 (10^{-3}X). We next attempted to use this approach to establish a selection strategy for cells that express elevated amounts of SLC5A6 from those that express it at lower levels.

3.2. SLC5A6 expression and B5 deprivation as a metabolic selection for transfected cell lines

We designed a B5-selection approach to select recombinant cells expressing the trastuzumab therapeutic immunoglobulin (IgG) or the green fluorescent protein (GFP) marker (Fig. 1C, Fig. S2A). CHO cells were co-transfected without (condition A) or with (conditions B and C) the SLC5A6 expression vector, together with the IgG or the GFP expression vectors along with a puromycin resistance marker. Subsequently, the culture was selected either in presence of puromycin (conditions A and B) or in the vitamin B5-deprived culture medium (10^{-3}X B5/10^{-4}X H, condition C). Control cells that had not been transfected with the SLC5A6 expression vector did not survive selection in the vitamin-deprived culture medium. After selection, cells were transferred into a non-selective medium until the analysis of the resulting polyclonal cell pools. Higher levels of IgG and GFP mRNAs and proteins were obtained from cells transfected with the SLC5A6 expression vector and selected using B5 deprivation, when compared to cells selected for puromycin resistance (Fig. 1D–F, Figs. S2B–E). Interestingly, single cell assays of GFP fluorescence indicated that condition C was capable of selecting cell populations displaying very high and homogeneous levels of transgene expression. Liquid-chromatography-mass spectrometry (LC-MS) metabolic analyses showed a decrease of lactate by-product after SLC5A6 overexpression and B5 deprivation (Fig. 1G). Ten IgG clones were randomly isolated by limiting dilutions of the polyclonal cell populations obtained from selection conditions B and C. The IgG secretion levels of clones obtained from cells selected using condition C were consistently higher than those of condition B (Figs. S3A and S3B). Two randomly-selected clones isolated from selection condition C displayed stable IgG secretion levels when maintained in complete non-selective medium for over two months of culture, indicating that a continuous selection for SLC5A6 expression is not required (Fig. S3C). Both clones showed comparable performance relative to a high-IgG expressor reference clone selected as the best among 192 clones, in terms of cell growth, viability and IgG secretion (Figs. S3D–F) illustrating the effectiveness of the novel selection process reported in this study. Overall, these data indicate that the cell selection process relying on SLC5A6 transporter expression and B5 selective medium provides consistent and homogeneous polyclonal populations, from which highly-expressing clones can be isolated at a high frequency.

The trastuzumab IgG is considered to be an “easy-to-express” (ETE) recombinant protein, as no major cellular bottleneck affects its production, with final yields in a bioreactor surpassing 1g/L. However, cells may struggle to produce high levels of recombinant IgG-fusion or chimeric proteins termed “difficult-to-express” (DTE), because of poorly understood metabolic limitations (Le Fourn et al., 2014). As the B5 selection process may be too stringent for cells struggling to express a DTE protein (termed hereafter DTE cells), we set up a milder B5-selection process by combining antibiotic and short (5 days) B5-deprivation selection of cells transfected with both antibiotic resistance and SLC5A6 selection vectors. This method was first assessed with ETE cells expressing the trastuzumab IgG (Fig. S4A). Cells subjected to the double antibiotic/B5 selection yielded more than 2-fold higher IgG production levels when compared to the single antibiotic selection (Fig. 2A; Fig. S4C), as mediated by the selective enrichment of a minor subpopulation of cells displaying very high IgG secretion levels (Fig. 2B). This effect required SLC5A6 overexpression, as expected (Figs. S4B and S4D). A similar enrichment of a minor subpopulation of cells expressing the transgene at highly elevated levels was also observed with GPF upon the double antibiotic/B5 selection of SLC5A6 overexpressing cells (Figs. S5 and S6). We next assessed whether this approach may be used to express the DTE TNFR-Fc fusion proteins, which consists of a chimeric protein comprising the receptor of the Tumor Necrosis Factor (TNFα) fused to the IgG constant chain (Fc). TNFR:Fc acts as a potent regulator of the inflammatory response resulting from autoimmune diseases, for which utilization as therapeutics is limited by very low levels of secretion, recovery and purification (Pybus et al., 2014). Cells were co-transfected with the puromycin and TNFR:Fc expression vectors or with these vectors plus SLC5A6, and were alternatively selected with puromycin and vitamin B5 limitation for 19 days (Fig. S7A). Recombinant cells subjected to the double antibiotic/B5 selection displayed much higher IgG secretion levels when compared to the cells subjected to antibiotic selection only (Fig. 2C–E; Figs. S7B and S7C). When the expression of the fusion protein was assessed in fed-batch cultures, the doubly selected cells displayed higher overall protein levels, despite lower cell numbers at the end of the culture time (Fig. 2F). Overall, these data indicated that SLC5A6 and vitamin B5-mediated selection can also be used in conjunction with antibiotic selection to

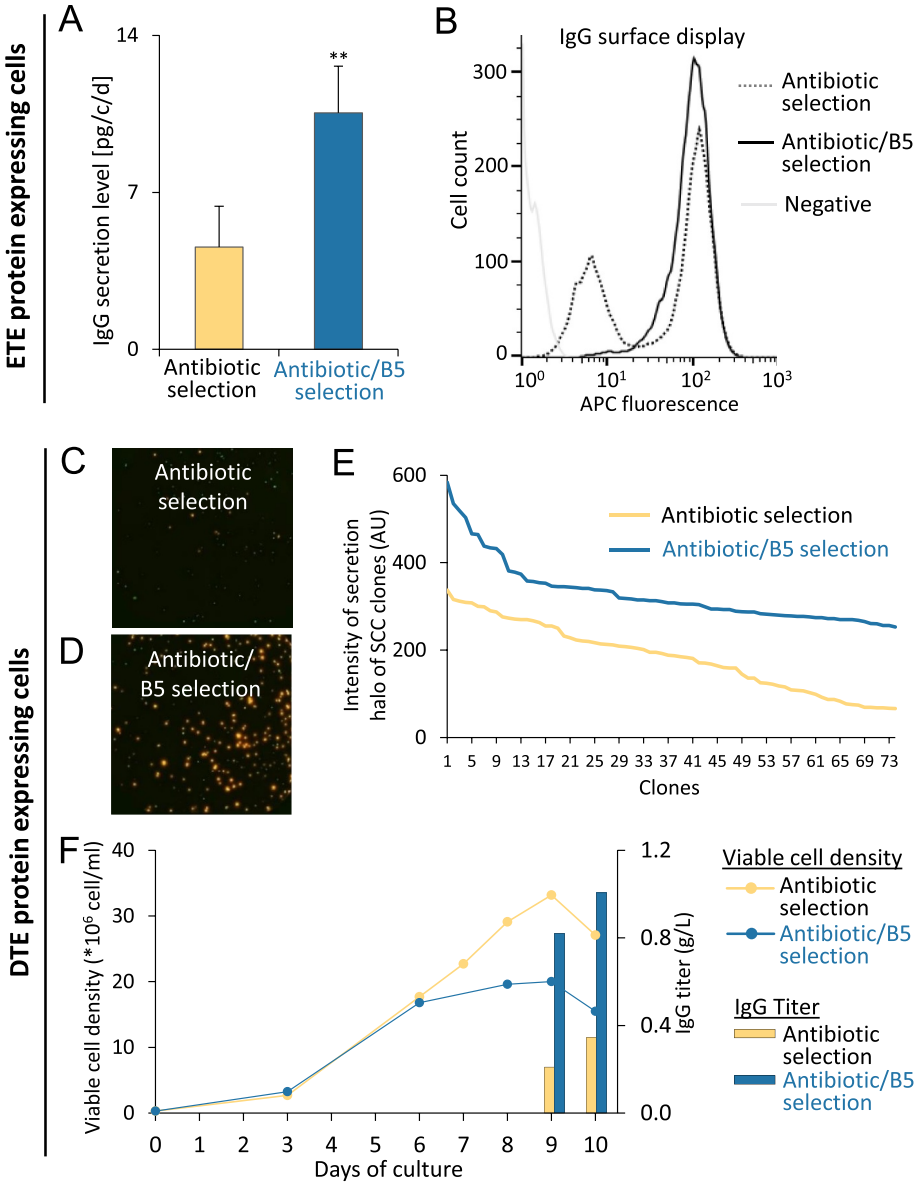

Fig. 2. Enrichment of ETE and DTE protein expressing cells by antibiotic and B5 double selection. (A–B) Cells were co-transfected with the ETE trastuzumab, *SLC5A6*, and puromycin resistance vectors, after which the culture was selected either in presence of puromycin, or by puromycin selection followed by 5 days of culture in B5-deficient medium. Selected cells were transferred to a non-selective culture medium followed by IgG secretion assays (A) and the analysis by cytofluorometry of IgG cell surface display assessed by immunofluorescence staining (B). Data are mean values ± SEM from 3 independent pools. $^{**}P \leq 0.02$ (*t*-test; 2 tails) vs. antibiotic selection. (C–F) Cells were co-transfected with or without the *SLC5A6* vector, and the DTE TNFR:Fc fusion and puromycin resistance vectors, after which the cultures were selected using puromycin only, or by consecutive selection steps performed using the B5-deficient medium and puromycin selection. Selected cells were transferred to a non-selective culture medium prior to analysis. (C–D) Cell secretion assay was used to assess the homogeneity and estimate the level of producing cells for puromycin- and puromycin/B5-selected pools. ClonePix FL Imager was used to rank and isolate cells according to their secretion halo intensity (E) and TNFR:Fc production assays were performed using fed-batch cultures of the clone with the highest secretion halo intensity obtained from puromycin- or puromycin/B5-selection (F).

preferentially select the cells that mediate the highest transgene expression levels, even when expressing DTE proteins that cannot be obtained at high levels using conventional selection methods.

3.3. B5 deprivation alters expression of PPAR-regulated lipid metabolism genes

The ability to express DTE proteins at high levels when using the vitamin B5 deprivation approach, and thus to bypass potential metabolic bottlenecks, suggested that this selection strategy may allow for the isolation of a minor fraction of variant cells bearing favourable genetic and/or epigenetic alterations. This was assessed using a RNA-seq transcriptomic analysis of cells producing the trastuzumab ETE or the beta-interferon DTE protein whose production is severely limited by protein aggregation (Han et al., 2009), comparing antibiotic/B5-, antibiotic- and non-selected cell populations (Fig. S8A). Genes whose expression was significantly upregulated in antibiotic/B5 vs. antibiotic selection in cells expressing either ETE and DTE proteins were selected for further analysis. Most selected genes displayed decreased expression after antibiotic-selection of recombinant protein-expressing cells, when compared to non-transfected cells (Figs. S8B and S8C). This effect was reversed or even overcompensated in antibiotic/B5-selected cells, along with the observed increase in recombinant protein expression. This suggested the possible occurrence of a cellular response caused by the recombinant protein itself or by the competition of its expression for limiting metabolic cellular functions after antibiotic selection. However, this effect would be suppressed upon B5 selection, if B5 deprivation may select cells having a persistently improved fitness and metabolism, and a correspondingly increased capacity for high level recombinant protein expression.

Among the 31 candidate genes selected as B5-selection targets, 14 were attributed to the biological activity or expression of the recombinant protein themselves, being categorized as immune response-associated (Fig. 3A; Table S1). Eleven were metabolic genes encoding enzymes and transporters, as might be expected from adaptive changes to their primary metabolism. Interestingly, five of these genes were involved in lipid metabolism, among which three, *HMGCS2*, *ACOT1* and *CYP4A14*, are known targets of PPARα (Rakhshandehroo et al., 2010). *Hydroxymethylglutaryl CoA synthase 2* (*HMGCS2*) encodes a mitochondrial protein that catalyses the first reaction of ketogenesis and controls the metabolic fate of fatty acids in the liver of starved animals (Vila-Brau et al., 2011). *ACOT1* encodes an acyl-CoA thioesterase

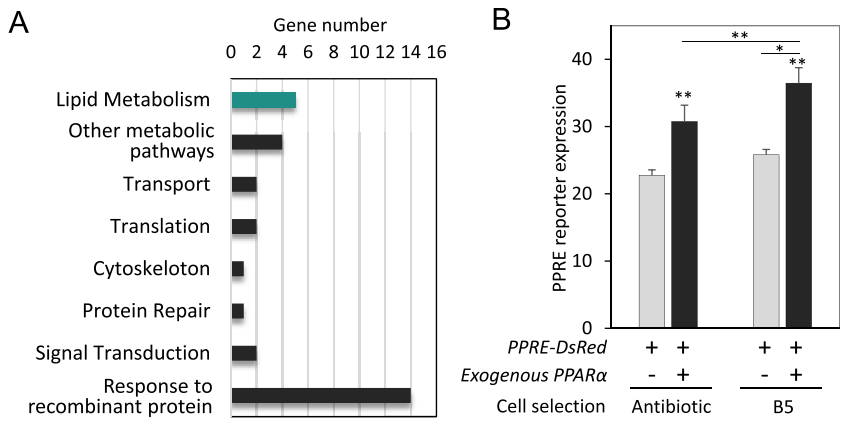

Fig. 3. PPARα activation studies in antibiotic- and B5-selected cells producing an ETE protein. (A) Ontological classes of the identified candidate genes whose expression may be persistently modified by limiting vitamin B5 selection. (B) Antibiotic-selected ETE cells and B5-selected ETE (trastuzumab) cells were transiently transfected with the PPRE-DsRed reporter, or cotransfected with the PPRE reporter and mouse PPARα cDNA. DsRed activity was standardized relative to BFP2 marker. Data represent mean fluorescence ± SEM of corrected DsRed activity from 4 replicates. $*P \leq 0.05$ and $**P \leq 0.02$ (*t*-test; 2 tails) with respect to antibiotic-selected cells without exogenous PPARα, unless otherwise indicated. Negative control of DsRed construct without PPRE is presented in supplemental data (S Fig. 9).

(CoASH) involved in long chain fatty-acid metabolism which catalyses the hydrolysis of acyl-CoAs to release free fatty acid and coenzyme A. CYP4A14 is a cytochrome P450 implicated in liver damage, inflammation, and fibrosis in mice (Zhang et al., 2007).

As PPARα mRNA levels were not persistently increased following antibiotic/B5 double selection, we next assessed whether the increase of PPARα target genes expression could result from the activation of this transcription factor by endogenous ligands that may be synthesized by B5-selected cells. B5-selected and antibiotic-selected cells were transfected with the PPRE-DsRed reporter of PPAR transcriptional activity with or without a PPARα expression vector, and DsRed fluorescence was assessed. Interestingly, exogenous expression of PPARα activated the PPAR responsive promoter to higher levels in B5- vs. antibiotic-selected cells (Fig. 3B; Fig. S9). Therefore, we hypothesized that B5 deprivation and the resulting starving stress may have yielded cells that persistently produce a PPARα agonist, and thus, that would express PPARα target genes at higher levels (Fig. S10).

3.4. PPAR activation improves cell resistance to stress

We next aimed to assess whether the gene expression changes induced by B5 starving and/or PPAR activation may result in reduced unhealthy by-products and/or improved cell metabolic fitness, thereby providing an explanation for their ability to efficiently express complex recombinant proteins. Bezafibrate (2-[4-[2-(4-chlorobenzamido)ethyl] phenoxy]-2-methylpropanoic acid) is a general PPAR pan-agonist used clinically as an anti-hyperlipidaemia drug (Inoue et al., 2002). Addition of bezafibrate to a fed batch culture of ETE protein-expressing cells induced the *HMGCS2* and *ACOT1* PPARα target genes, as well as several other known PPAR targets such as DBI1, ASCL1 and the RXR nuclear receptor (Rakhshandehroo et al., 2010) (Fig. 4A). Interestingly, another B5-selection induced gene, *SLC22A14*, was also activated in response to bezafibrate. While the SLC22A14 transporter has been linked to sperm mobility and fertility in mice (Maruyama et al., 2016), a potential PPAR-associated function has not been described as yet, although a PPRE regulatory sequence was identified upstream of its gene (Tzeng et al., 2015). Bezafibrate was added to the cells at day 3, during the culture exponential phase, and its effect on cell growth and IgG secretion was observed up to 10 days of fed or non-fed cultures. When the cells were subjected to a feeding stress, by omitting the addition of feed supplements to the cell culture, bezafibrate-treated cells survived and kept secreting the IgG, whereas non-treated cells rapidly died (Fig. 4B). In contrast, upon feeding, cells growth and IgG production were rather decreased by bezafibrate addition. Thus, we concluded that the induction of PPAR target genes by bezafibrate was beneficial in cell stress conditions linked to nutrient deprivation, supporting a role for PPAR in maintaining cell fitness and energy homeostasis, and/or in reducing the accumulation of toxic metabolic by-products such as lactate.

3.5. PPAR activation affects lipid metabolism and improves recombinant protein secretion

To assess the effect of PPARα on cell metabolism, antibiotic-selected clones expressing the trastuzumab ETE protein were transfected with a mouse PPARα cDNA expression vector. Cells stably overexpressing the transcription factor were selected for resistance to another antibiotic. The resulting ETE clones overexpressing PPARα displayed elevated expression of *HMGSC2*, *ACOT1*, *CYP4A14* and *SLC22A14* genes, suggesting that intracellular PPAR agonists were available in the cells to activate the exogenous PPARα (Fig. S11). Interestingly, the PPARα-overexpressing clones showed an improved IgG specific production compared to control clones, yielding a 30% increase of the titers, to over 2 g/L (Fig. 5A and B). This indicated that activation of PPAR target genes by either the B5 selection approach or by PPARα overexpression yielded similar improvements of the cells' ability to express the recombinant protein at high levels.

A DTE cell clone transfected to overexpress PPARα similarly increased recombinant protein productivity, and this increase was further amplified by a five days B5-deprivation treatment, indicating that the two approaches may be combined to further boost recombinant protein production (Fig. 5C; Fig. S12). Metabolite quantification of these PPARα overexpressing cells indicated decreased intracellular concentrations of vitamin B5, lactate and the ketone body 3-HB and an increase in acetyl-CoA (Fig. 5D–G). Since vitamin B5 is a precursor of acetyl-CoA, this indicated that PPARα overexpressing cells may have an accelerated turnover of the vitamin, thus providing more acetyl-CoA, as required for cellular energy production by the Krebs cycle, as well as for lipid metabolism (Fig. S13). Thus, we concluded that activation of PPARs and their target genes by a fasting state induced by vitamin B5 deprivation and/or by PPARα overexpression, may collectively modulate metabolite balances by decreasing the production of toxic lactate by-products, as well as by altering lipid metabolism and the synthesis of derived ketones bodies. This may in turn improve cell fitness, leading to an increased capacity to produce the recombinant protein of interest.

4. Conclusion

In the present work, we first aimed to capitalize on mammalian cell dependence on vitamin B5 for central metabolism balance, in order to select cells with improved fitness and energy homeostasis, as required to efficiently express complex therapeutic proteins. We established a selective metabolic procedure based on a SLC5A6 multivitamin transporter and vitamin B5 deprivation, providing a powerful selection for cells expressing transgenes at high levels, either alone or in combination with other selection procedures. Unlike other processes based on the selection of cells with the spontaneous co-amplification of the selection marker and of the transgene of interest, such as in the DHFR metabolic selection (Cacciatore et al., 2010), use of the SLC5A6-based

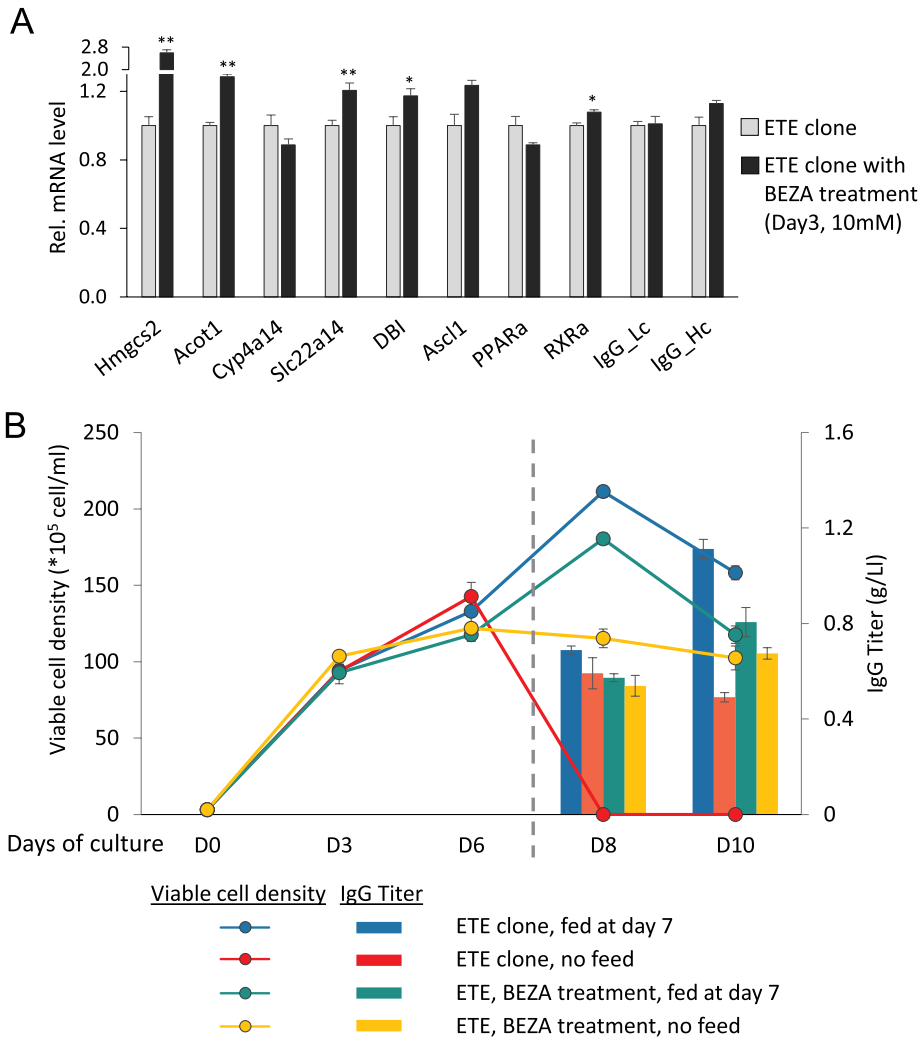

Fig. 4. PPAR activation studies in an ETE protein-producing clone. (A) A clone producing the ETE trastuzumab was treated or not with 10 mM bezafibrate (BEZA) after 3 days of fed batch culture, and candidate gene mRNA levels were quantified at Day 6 using RT-qPCR. $^{*}P \leq 0.05$, $^{**}P \leq 0.02$ (*t*-test; 2 tails) vs. the culture devoid of bezafibrate. (B) Cell viability was measured from Day 0 to Day 10 of fed batch cultures treated as for panel A, with or without the addition of a feed at day 7 (dashed grey line), and the titer of IgG secreted in the cell supernatant was assessed at Day 8 and 10 by sandwich ELISA. Averages ± SEM of values from 3 replicates are shown.

selection process does not require lengthy gene amplification steps, and it yielded stable levels of expression after the removal of the selection pressure. The B5 selection does not require the cells to acquire a resistance to toxic compounds such as antibiotics, and it has a potential for use in the field of gene and cell therapy, as it may face fewer ethical or safety issues than traditional methods.

We showed that B5-deprivation or PPARα overexpression alone were effective to improve cell recombinant protein production, but that a combination of the two further enhanced this effect. We provide evidence that cells transiently deprived of vitamin B5 may have acquired persistent alterations in their lipid metabolism, as mediated by the activation of PPARα transcription factor. Using the general chemical PPAR agonist bezafibrate, we showed that PPAR signalling activation can protect cells from dying upon a stress caused by feeding deprivation. Overall, we propose a role for PPARs in the maintenance of central cellular energy balance, in improved cell fitness and in reduced synthesis of toxic metabolism by-products. These effects may combine to allow increased production of recombinant proteins, including difficult-to-express proteins known to elicit detrimental cellular stress responses (Fig. S14). Further analysis of the changes in metabolic fluxes activated by the PPAR and by the fasting process will be required to decipher the mechanisms behind those metabolic alterations and what their relative contributions may be to increasing cell fitness (Pourcel et al., 2020; Berger et al., 2020). So far, the PPAR activation and signalling pathway has been mainly studied at the whole organism level, PPAR being expressed and activated in specific tissues (*e.g.* liver cells for PPARα) to act distantly, for instance by providing the required substrate for energy production by muscle fibers. Here, we show that PPARs may control important functions in other cell types such as cultured ovary cells, allowing them to maintain a high fitness when subjected to the metabolic stress conditions of fed batch cultures, when the cells reach high densities and mediate elevated protein production levels.

As the PPARs are known to be activated upon food starvation, we hypothesize that B5 deprivation led to a fasting state of the cells, resulting in the production of one or several as yet unknow PPAR ligands. The synthesis of such ligand would persist even after B5 deprivation is terminated and cells are grown in complete medium, thus explaining the observed persistent activation of PPAR target gene expression. This event might thus be considered as a cellular memory of the deprivation state, providing increased resistance to further potential fasting events. In other words, our results imply that cultured cells, once exposed to metabolic starvation, may display an improved metabolic fitness as compared to non-exposed cells, allowing increased resistance to cellular stresses. However, whether this may stem from e.g. epigenetic changes specifically elicited by the fasting state, or by the fast selection of a minority of pre-existing cells having spontaneously increased PPAR signalling, and thus surviving selection by the starvation stress, remains to be established.

Author contributions

L.P. and N.M. designed the project; L.P., V.L., P.A.G., F.B; M.D. and F.G. performed the experiments; L.P analysed the data and L.P. and

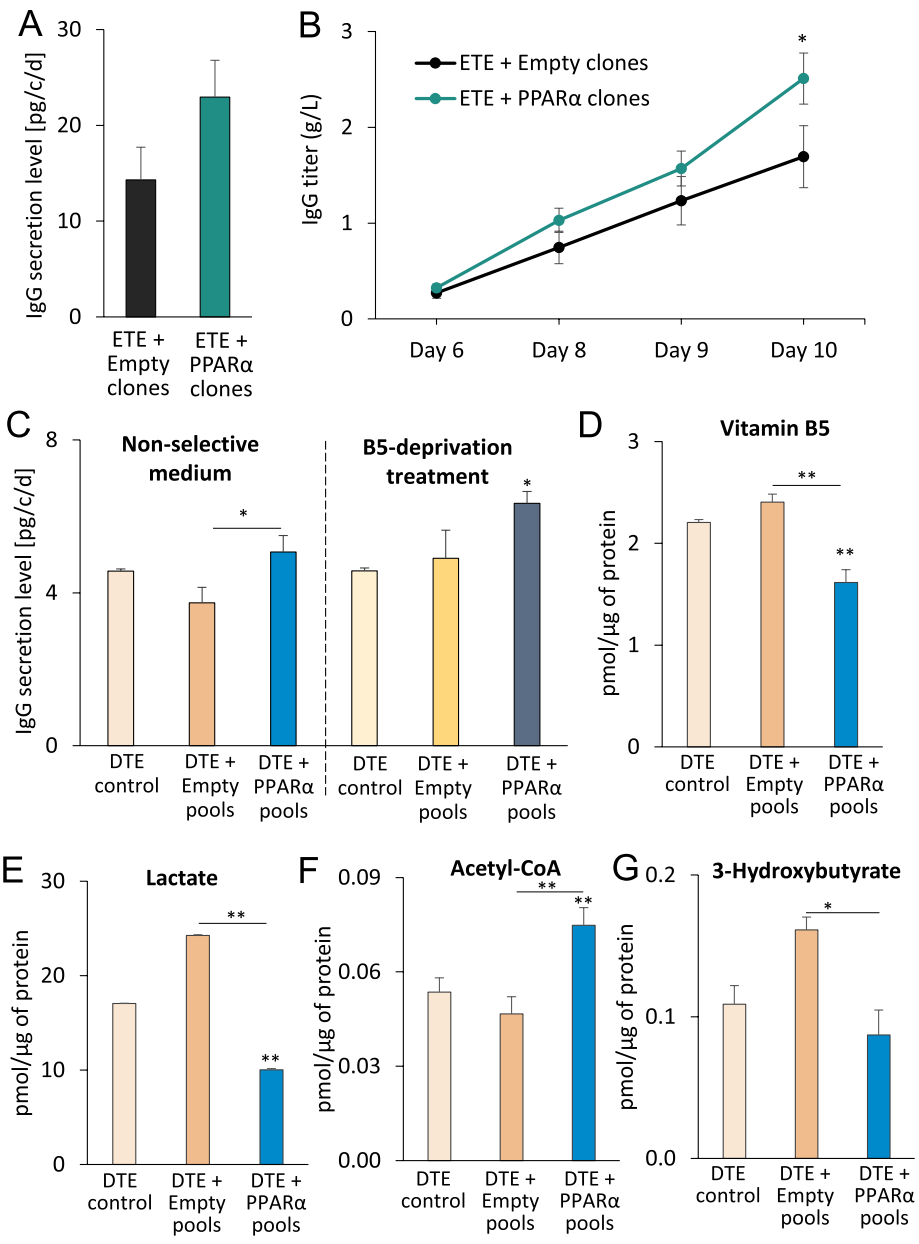

Fig. 5. PPARα overexpression in ETE and DTE-producing cellsAnt. ibiotic-selected clone ETE (trastuzumab) and DTE (infliximab) were stably transfected with mouse PPARα or with an empty vector, and the resulting stable cell pools and derived clones were used for further analysis. (A) IgG specific productivity and (B) IgG production levels of ETE-selected clones in fed-batch culture conditions. Data are means ± SEM from 4 to 6 independent clones. $^{*}P \leq 0.05$, $^{**}P \leq 0.02$ (*t*-test; 1 tail) with respect to the control. (C) DTE stable cell pools were subjected to 5 days of B5-starving treatment, then transferred to non selective media before being analysed for IgG secretion level. IgG specific productivity was measured over 3 days of culture in non-selective medium. Data are means ± SEM from 2 to 3 replicates. $^{*}P \leq 0.05$ (*t*-test; 2 tails) with respect to the control not subjected with B5-starvation, unless otherwise indicated. (D–G) Metabolic content in DTE cell pool transfected with an empty vector or PPARα, after 6 days of a fed-batch culture, measured by LC-MS. Data are means ± SEM from 3 replicates. $^{*}P \leq 0.05$, $^{**}P \leq 0.02$ (*t*-test; 2 tails) with respect to the control, unless otherwise indicated.

N.M. wrote the paper.

Declaration of competing interest

Some of the authors are employed by Selexis SA, a company that generates CHO cell clones expressing therapeutic proteins.

Acknowledgements

We thank the Metabolomics Platform at University of Lausanne for the metabolic analyses and the Swiss Institute of Bioinformatics for RNA sequencing raw data analyses. This work was supported by the University of Lausanne and a grant from the Swiss Government Commission for Technology and Innovation (grant 13939.1 PFLS-LS) and Selexis SA.

Appendix A. Supplementary data

Supplementary data to this article can be found online at https://doi.org/10.1016/j.ymben.2020.03.008.

References

Berger, A., Le Fourn, V., Masternak, J., Regamey, A., Bodenman, I., Girod, P., Mermod, N., 2020. Overexpression of transcription factor Foxa1 and target genes remediate therapeutic protein production bottlenecks in Chinese hamster ovary cells. Biotechnol. Bioeng. 4, 1101–1116.

Brezinsky, S.C.G., Chiang, G.G., Szilvasi, A., Mohan, S., Shapiro, R.I., MacLean, A., Sisk, W., Thill, G., 2003. A simple method for enriching populations of transfected CHO cells for cells of higher specific productivity. J. Immunol. Methods 277, 141–155.

Cacciatore, J.J., Chasin, L.A., Leonard, E.F., 2010. Gene amplification and vector engineering to achieve rapid and high-level therapeutic protein production using the Dhfr-based CHO cell selection system. Biotechnol. Adv. 28, 673–681.

Dean, J., Reddy, P., 2013. Metabolic analysis of antibody producing CHO cells in fed-batch production. Biotechnol. Bioeng. 110, 1735–1747.

Ghosal, A., Lambrecht, N., Subramanya, S.B., Kapadia, R., Said, H.M., 2013. Conditional knockout of the Slc5a6 gene in mouse intestine impairs biotin absorption. Am. J. Physiol. Gastrointest. Liver Physiol. 304, G64–G71.

Han, Y.K., Koo, T.Y., Lee, G.M., 2009. Enhanced interferon-beta production by CHO cells through elevated osmolality and reduced culture temperature. Biotechnol. Prog. 25, 1440–1447.

Harraghy, N., Buceta, M., Regamey, A., Girod, P.A., Mermod, N., 2012. Using matrix attachment regions to improve recombinant protein production. In: In: Hartley, J.L.

(Ed.), Protein Expression in Mammalian Cells: Methods and Protocols 801. Humana Press Inc, Totowa, pp. 93–110.
Inoue, I., Itoh, F., Aoyagi, S., Tazawa, S., Kusama, H., Akahane, M., Mastunaga, T., Hayashi, K., Awata, T., Komoda, T., Katayama, S., 2002. Fibrate and statin synergistically increase the transcriptional activities of PPARalpha/RXRalpha and decrease the transactivation of NFkappaB. Biochem. Biophys. Res. Commun. 290, 131–139.
Issemann, I., Green, S., 1990. Activation of a member of the steroid hormone receptor superfamily by peroxisome proliferators. Nature 347, 645–650.
Kersten, S., Desvergne, B., Wahli, W., 2000. Roles of PPARs in health and disease. Nature 405, 421–424.
Kobayashi, D., Kusama, M., Onda, M., Nakahata, N., 2011. The effect of pantothenic acid deficiency on keratinocyte proliferation and the synthesis of keratinocyte growth factor and collagen in fibroblasts. J. Pharmacol. Sci. 115, 230–234.
Kotas, M.E., Medzhitov, R., 2015. Homeostasis, inflammation, and disease susceptibility. Cell 160, 816–827.
Le Fourn, V., Girod, P.A., Buceta, M., Regamey, A., Mermod, N., 2014. CHO cell engineering to prevent polypeptide aggregation and improve therapeutic protein secretion. Metab. Eng. 21, 91–102.
Lee, J.M., Wagner, M., Xiao, R., Kim, K.H., Feng, D., Lazar, M.A., Moore, D.D., 2014. Nutrient-sensing nuclear receptors coordinate autophagy. Nature 516, 112–115.
Lindhurst, M.J., Fiermonte, G., Song, S., Struys, E., De Leonardis, F., Schwartzberg, P.L., Chen, A., Castegna, A., Verhoeven, N., Mathews, C.K., Palmieri, F., Biesecker, L.G., 2006. Knockout of Slc25a19 causes mitochondrial thiamine pyrophosphate depletion, embryonic lethality, CNS malformations, and anemia. Proc. Natl. Acad. Sci. U. S. A. 103, 15927–15932.
Maruyama, S.Y., Ito, M., Ikami, Y., Okitsu, Y., Ito, C., Toshimori, K., Fujii, W., Yogo, K., 2016. A critical role of solute carrier 22a14 in sperm motility and male fertility in mice. Sci. Rep. 6, 36468.
Newman, J.C., Covarrubias, A.J., Zhao, M., Yu, X., Gut, P., Ng, C.P., Huang, Y., Haldar, S., Verdin, E., 2017. Ketogenic diet reduces midlife mortality and improves memory in aging mice. Cell Metabol. 26, 547–557 e8.
Pietrocola, F., Galluzzi, L., Bravo-San Pedro, J.M., Madeo, F., Kroemer, G., 2015. Acetyl coenzyme A: a central metabolite and second messenger. Cell Metabol. 21, 805–821.
Pourcel, L., Buron, F., Arib, G., Le Fourn, V., Regamey, A., Bodenmann, I., Girod, P., Mermod, N., 2020. Influence of cytoskeleton organization on recombinant protein expression by CHO cells. Biotechnol. Bioeng. 4, 1117–1126.
Pruitt, K.D., et al., 2014. RefSeq: an update on mammalian reference sequences. Nucleic Acids Res. 42, 756–763.
Puchalska, P., Crawford, P.A., 2017. Multi-dimensional roles of ketone bodies in fuel metabolism, signaling, and therapeutics. Cell Metabol. 25, 262–284.
Pybus, L.P., Dean, G., West, N.R., Smith, A., Daramola, O., Field, R., Wilkinson, S.J., James, D.C., 2014. Model-directed engineering of "difficult-to-express" monoclonal antibody production by Chinese hamster ovary cells. Biotechnol. Bioeng. 111, 372–385.
Rakhshandehroo, M., Knoch, B., Müller, M., Kersten, S., 2010. Peroxisome proliferator-activated receptor alpha target genes. PPAR Res. 2010, 20.
Redman, L.M., Smith, S.R., Burton, J.H., Martin, C.K., Il'yasova, D., Ravussin, E., 2018. Metabolic slowing and reduced oxidative damage with sustained caloric restriction support the rate of living and oxidative damage theories of aging. Cell Metabol. 27, 805–815 e4.
Subramanian, V.S., Subramanya, S.B., Said, H.M., 2012. Relative contribution of THTR-1 and THTR-2 in thiamin uptake by pancreatic acinar cells: studies utilizing Slc19a2 and Slc19a3 knockout mouse models. Am. J. Physiol. Gastrointest. Liver Physiol. 302, G572–G578.
Tzeng, J., Byun, J., Park, J.Y., Yamamoto, T., Schesing, K., Tian, B., Sadoshima, J., Oka, S., 2015. An ideal PPAR response element bound to and activated by PPARalpha. PloS One 10, e0134996.
Uchida, Y., Ito, K., Ohtsuki, S., Kubo, Y., Suzuki, T., Terasaki, T., 2015. Major involvement of Na + -dependent multivitamin transporter (SLC5A6/SMVT) in uptake of biotin and pantothenic acid by human brain capillary endothelial cells. J. Neurochem. 134, 97–112.
van den Berghe, G., 1991. The role of the liver in metabolic homeostasis: implications for inborn errors of metabolism. J. Inherit. Metab. Dis. 14, 407–420.
Vila-Brau, A., De Sousa-Coelho, A.L., Mayordomo, C., Haro, D., Marrero, P.F., 2011. Human HMGCS2 regulates mitochondrial fatty acid oxidation and FGF21 expression in HepG2 cell line. J. Biol. Chem. 286, 20423–20430.
Zhang, Y.M., Chohnan, S., Virga, K.G., Stevens, R.D., Ilkayeva, O.R., Wenner, B.R., Bain, J.R., Newgard, C.B., Lee, R.E., Rock, C.O., Jackowski, S., 2007. Chemical knockout of pantothenate kinase reveals the metabolic and genetic program responsible for hepatic coenzyme A homeostasis. Chem. Biol. 14, 291–302.